

# Magnetic quantum tunneling in $\text{Ca}_3\text{Co}_2\text{O}_6$ studied by ac susceptibility: Temperature and magnetic-field dependence of the spin-relaxation time

V. Hardy and D. Flahaut

*Laboratoire CRISMAT, UMR 6508, Boulevard du Maréchal Juin, 14050 Caen Cedex, France*

M. R. Lees and O. A. Petrenko

*Department of Physics, University of Warwick, Coventry, CV4 7AL, United Kingdom*

(Received 20 July 2004; revised manuscript received 22 October 2004; published 30 December 2004)

The geometrically frustrated spin-chain compound  $\text{Ca}_3\text{Co}_2\text{O}_6$  was recently found to exhibit properties suggesting the phenomenon of quantum tunneling of the magnetization (QTM). The present paper addresses this issue by investigating the temperature and magnetic-field dependence of the characteristic spin-relaxation time  $\tau$ . This study is based on the analysis of the out-of-phase ac magnetic susceptibility of single crystals. The overall behavior is found to support the occurrence of QTM in  $\text{Ca}_3\text{Co}_2\text{O}_6$ : (i) saturation of  $\tau$  at low  $T$ ; (ii) observation of identical  $\tau$  values in the magnetic fields corresponding to the steps in the  $M$  vs  $H$  curve at low  $T$ ; (iii) existence of a dip centered at zero field in the  $\tau$  vs  $H$  curve at low  $T$ . These QTM-like features found in  $\text{Ca}_3\text{Co}_2\text{O}_6$  are compared to those previously reported in other materials such as single-molecular magnets.

DOI: 10.1103/PhysRevB.70.214439

PACS number(s): 75.60.-d, 75.45.+j

## I. INTRODUCTION

Geometrically frustrated magnetic materials have attracted considerable attention in recent years, owing to the peculiar properties that are often displayed by these systems.<sup>1</sup> Most of the studies reported so far have been carried out on three-dimensional or two-dimensional systems (pyrochlore and Kagomé-like structures, respectively). Geometrical frustration, however, can also be found in one-dimensional systems, namely, Ising-like chains, when they are arranged on a hexagonal lattice with an antiferromagnetic interchain coupling.<sup>2</sup> It was recently emphasized that this particular situation is encountered in some members of the family of oxides of general formula  $A'_3\text{ABO}_6$ , where  $A'$  is Ca or Sr, while  $A$  and  $B$  can be transition metal elements.<sup>3</sup> One of this family of compounds that has been intensively studied is  $\text{Ca}_3\text{Co}_2\text{O}_6$ .<sup>4-17</sup>

The structure of  $\text{Ca}_3\text{Co}_2\text{O}_6$  consists of chains made up of  $\text{CoO}_6$  trigonal prisms alternating with  $\text{CoO}_6$  octahedra, which run along the  $c$  axis of the hexagonal cell.<sup>4</sup> These chains are separated by the Ca ions and they form a hexagonal lattice on the  $ab$  plane. Although it remains a matter for debate, the Co ions are usually reported to be trivalent for both sites.<sup>5,7,8,18</sup> Owing to the difference in the crystalline electric field (CEF) on the two sites, the  $\text{Co}^{3+}(3d^6)$  ions are expected to be in the high-spin state for the prismatic sites and in the low-spin state for the octahedral sites.<sup>5</sup> Each magnetic chain along  $c$  can thus be seen as an alternation between  $S=2$  and  $S=0$ , with the spins oriented along the chain direction. The intrachain coupling  $J$  is ferromagnetic and using an exchange Hamiltonian of the form  $-2JS_iS_j$ , analysis of the paramagnetic regime leads to  $J \sim 15$  K,<sup>7</sup> while the interchain coupling  $J'$  is antiferromagnetic and weaker (the field-induced transition to the ferromagnetic state at low  $T$  suggests that  $J' \sim -0.2$  K).<sup>17</sup>

As  $T$  is decreased in zero field, a long-range magnetic ordering takes place at  $T_N \approx 26$  K.<sup>5</sup> Owing to the geometrical

frustration, however, this order is not complete. The most likely configuration is the onset of a “partially disordered antiferromagnetic” (PDA) state,<sup>6,19</sup> where two-thirds of the ferromagnetic chains are coupled antiferromagnetically, while the remaining third are incoherent (disordered chains with zero net magnetization).<sup>20</sup> As  $T$  is lowered below  $T_N$ , short-range ordering progressively develops along the incoherent chains, until the appearance of a spin-freezing phenomenon around  $T_{\text{SF}} \sim 7-8$  K.<sup>6,11,12</sup> No other transition is observed down to 2 K. Within the range  $T_{\text{SF}} < T < T_N$ , the application of a magnetic field along  $c$  breaks the frustration and leads to the onset of a ferrimagnetic state<sup>5-8</sup> characterized by a magnetization plateau at  $M_S/3$  ( $M_S$  is the saturation magnetization  $\sim 4.8 \mu_B/\text{f.u.}$ ). Increasing the magnetic field still further leads to a jump in magnetization from  $M_S/3$  to  $M_S$  at  $H_C \approx 3.6$  T, which was ascribed to the transition between the ferrimagnetic and ferromagnetic states.<sup>5-8</sup> For  $T < T_{\text{SF}}$ , hysteresis appears on the  $M(H)$  curves and the field-induced plateau at  $M_S/3$  is progressively replaced by a succession of magnetization steps with a roughly constant field spacing ( $\mu_0\Delta H \sim 1.2$  T).<sup>7,8,21</sup> This is one of the features that has led us to discuss the possible occurrence of a quantum tunneling of the magnetization (QTM) in  $\text{Ca}_3\text{Co}_2\text{O}_6$ .<sup>21</sup>

This tunneling process corresponds to a reversal of the spin direction across the energy barrier associated with the CEF-induced single-ion anisotropy.<sup>22,23</sup> In a first approximation, QTM is expected to take place in resonant magnetic fields given by  $\mu_0 H = n(D/g\mu_B)$ , where  $n$  is an integer,  $D$  the single-ion anisotropy, and  $g$  the Landé factor. In recent years, QTM has been intensively studied in single-molecular magnets (SMM's), such as  $[\text{Mn}_{12}(\text{CH}_3\text{COO})_{16}(\text{H}_2\text{O})_4\text{O}_{12}] \cdot 2\text{CH}_3\text{COOH} \cdot 4\text{H}_2\text{O}$  (usually referred to as  $\text{Mn}_{12}$ ).<sup>23,24</sup> These molecular systems are particularly suitable for the study of QTM because they constitute dense collections of identical and independent magnetic particles having a large spin and a sizable uniaxial anisotropy (e.g.,  $S=10$  and  $D \sim 0.6$  K for  $\text{Mn}_{12}$ ).<sup>23,24</sup> Recently, some in-

dications of a QTM process were reported in very different materials, namely, the oxides  $\text{Ho}_2\text{Ti}_2\text{O}_7$  (Ref. 25) and  $\text{Dy}_2\text{Ti}_2\text{O}_7$ .<sup>26</sup> It is worth noting that these “spin ice” materials and  $\text{Ca}_3\text{Co}_2\text{O}_6$  are systems exhibiting geometrical frustration as well as a large single-ion anisotropy. A peculiarity of  $\text{Ca}_3\text{Co}_2\text{O}_6$  is that the signatures of QTM were found at  $T \ll T_N$ , which is puzzling at first glance. It must be kept in mind, however, that the ordering at  $T_N$  is only partial since one-third of the chains are left incoherent in the PDA state. This situation clearly illustrates how geometrical frustration can favor the development of QTM in crystalline systems, by allowing the persistence of magnetic degrees of freedom at low  $T$  (in our case, the existence of “free” chains embedded in an ordered matrix).<sup>27</sup>

At present, however, it must be recognized that the very existence of QTM in  $\text{Ca}_3\text{Co}_2\text{O}_6$  is still a matter for debate. Therefore, in order to provide additional data addressing this issue, we carried out a detailed investigation of the low- $T$  spin dynamics in  $\text{Ca}_3\text{Co}_2\text{O}_6$  single crystals. The study reported in the present paper was based on ac susceptibility data taken as a function of frequency ( $f$ ), temperature ( $T$ ), and dc magnetic field ( $\mu_0 H$ ).

## II. EXPERIMENTAL DETAILS

Single crystals of  $\text{Ca}_3\text{Co}_2\text{O}_6$  were grown by heating a mixture of  $\text{Ca}_3\text{Co}_4\text{O}_9$  and  $\text{K}_2\text{CO}_3$ , in a weight ratio of 1/7, at 950 °C for 50 h in an alumina crucible in air. The cooling is performed in two steps, first down to 930 °C at 10 °C/h and then down to room temperature at 100 °C/h. We took crystals having a needlelike shape with the longest dimension (typically 4 mm) along  $c$ . Because of their small size, we used an assembly of 13 crystals (giving a total mass  $\sim 27$  mg). The ac susceptibility measurements (in phase  $\chi'$  and out of phase  $\chi''$ ) were recorded by means of a superconducting quantum interference device—(SQUID-)based commercial device (Quantum Design), with a constant excitation field of  $h_{ac}=3$  Oe, and frequencies ranging from 0.01 to 1000 Hz. Measurements were carried out at temperatures down to 2 K and in dc magnetic fields up to a few teslas. The single crystals were optically aligned with their  $c$  axis oriented along the magnetic fields (ac and dc). The data were recorded either versus temperature at a fixed frequency or versus frequency at a fixed temperature. All the measurements in nonzero dc magnetic fields were recorded after a zero-field cooling from 35 K  $\gg T_N$ . The curves registered in zero field as a function of the temperature were recorded upon cooling from  $T > T_N$ . The effective cooling rate for these measurements was quite low (i.e.,  $\sim 1.5$  K/h). We note that curves obtained when increasing the temperature after such a procedure were found to be superimposed on those recorded upon cooling. The curves registered in zero field as a function of the frequency were recorded by starting from 0.1 Hz. Then, it typically took 1 h to scan the frequency up to 1000 Hz. For each curve, the crystals were first warmed up to  $T > T_N$  and then directly cooled down to the desired temperature. As a result, the effective cooling rate for the  $\chi(f)$  curves was substantially larger than for the  $\chi(T)$  curves (e.g., the cooling down to 2 K typically took 1 h in the former case instead of 20 h in the latter).

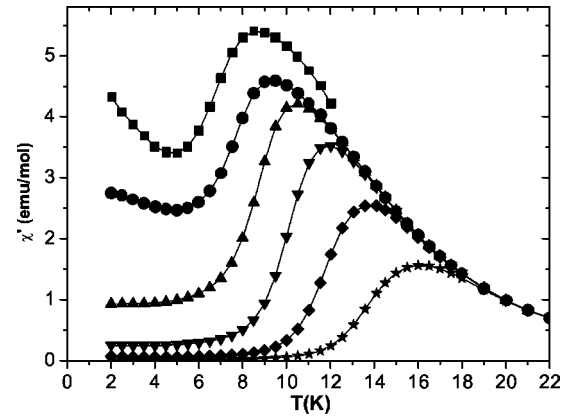


FIG. 1.  $\chi'$  data in zero field, recorded at different frequencies: 0.01 Hz (squares), 0.1 Hz (circles), 1 Hz (triangles up), 10 Hz (triangles down), 100 Hz (diamonds), 1000 Hz (stars).

## III. RESULTS

Figure 1 shows  $\chi'(T)$  curves recorded in zero field at different frequencies between 0.01 and 1000 Hz. This data set is in qualitative agreement with the previous results obtained in crystals<sup>8</sup> and ceramics.<sup>13</sup> Beyond a large shift with frequency in the location of the peak, a peculiar behavior is observed at low temperatures: as the frequency is decreased, there is a substantial increase in the susceptibility accompanied by the appearance of an upward curvature in  $\chi'(T)$ . Such features point to an intriguing change in the spin dynamics within this low  $T$  range. In the present paper, we have focused on the  $\chi'$  data which allow a direct extraction of the characteristic spin-relaxation time. Figure 2 shows  $\chi''$  curves in zero field, which were recorded either versus temperature at constant frequency (top panel) or versus frequency at constant temperature (bottom panel). We note that the present  $\chi''(T)$  curves are consistent with the previous data ( $f \geq 1$  Hz) obtained on single crystals.<sup>8</sup> As a general rule,<sup>28</sup> a peak in  $\chi''(T)$  or  $\chi''(f)$  corresponds to a situation where the characteristic spin-relaxation time  $\tau$  is equal to the characteristic time of the measurement ( $1/2\pi f$ ). In the course of the study, we realized that the location of the peaks in  $\chi''(T)$  or  $\chi''(f)$  can be substantially affected by the time spent at low  $T$ . Figure 3 illustrates this effect in the case of  $\chi''(f)$  by showing—at three different temperatures—the curves recorded after a waiting time equal to 0, 2, or 4 h. This effect of time was found to be substantial only within the range  $T \sim 10 \pm 2$  K.

When comparing the data of Figs. 2(a) and 2(b), one can observe significant differences in the value of  $\chi''$  for certain combinations of temperature and frequency. For 1000 Hz, the agreement between both sets of data is excellent at all temperatures, and it remains quite good for 100 Hz. For lower frequencies, however, a discrepancy appears at  $T \leq 10$  K. In the range 8–10 K, we suggest that this difference can be ascribed to an effect of relaxation. It was shown in Fig. 3 that  $\chi''$  increases significantly with time in the range  $10 \pm 2$  K, for frequencies lower than  $\sim 50$  Hz. Since the cooling rate is much slower for the  $\chi''(T)$  curves than for the

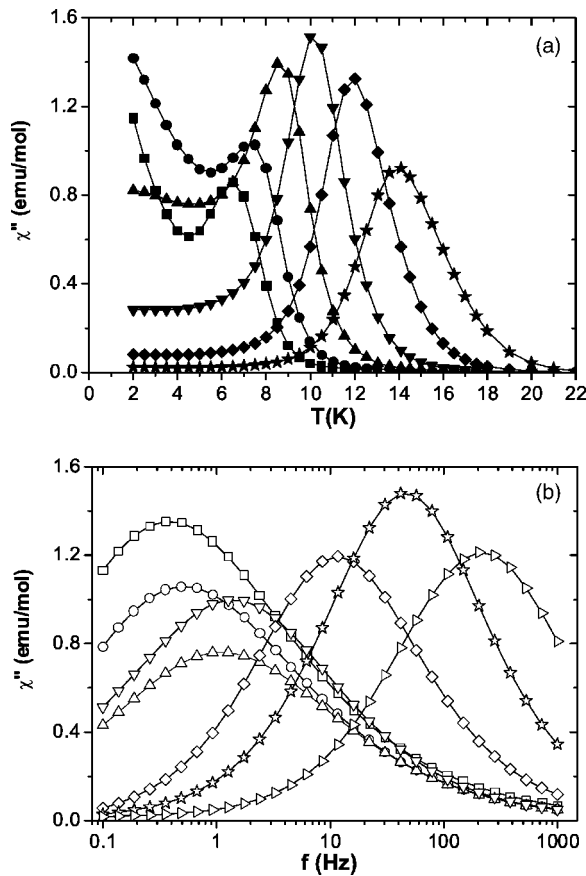


FIG. 2.  $\chi''$  data in zero field. (a)  $\chi''(T)$  curves recorded at different frequencies: 0.01 Hz (squares), 0.1 Hz (circles), 1 Hz (triangles up), 10 Hz (triangles down), 100 Hz (diamonds), 1000 Hz (stars). (b)  $\chi''(f)$  curves recorded at different temperatures: 2.25 K (squares), 3.5 K (circles), 6 K (triangles up), 8 K (triangles down), 10 K (diamonds), 11.5 K (stars), 13 K (triangles right).

$\chi''(f)$  ones, the influence of this relaxation must be more visible in the former case, which might explain the larger  $\chi''$  values seen in Fig. 2(a) (at 8 and 10 K, for  $f \leq 10$  Hz). On the other hand, variations in  $\chi''$  between Figs. 2(a) and 2(b)

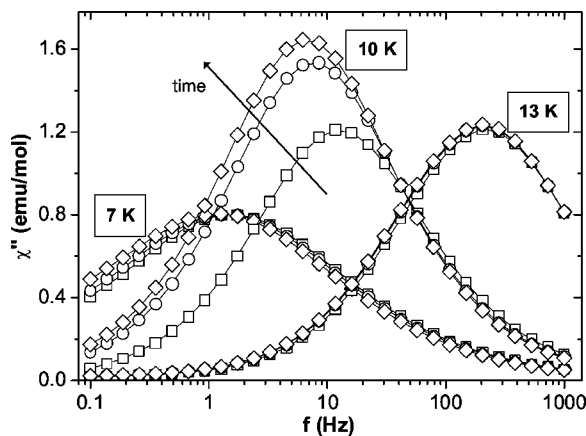


FIG. 3.  $\chi''(f)$  curves at three temperatures in zero field. At each temperature, curves were recorded after a waiting time equal to zero (squares), 2 h (circles), and 4 h (diamonds).

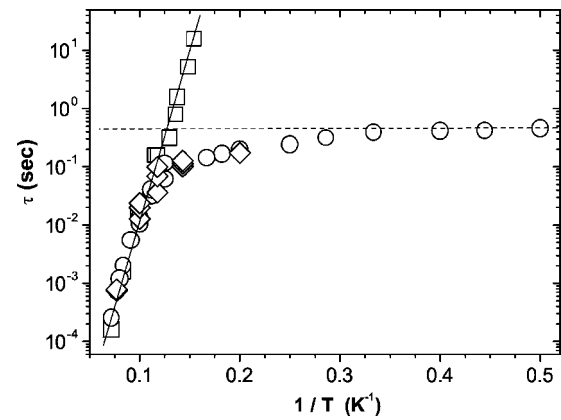


FIG. 4. Temperature dependence of the characteristic spin-relaxation time in zero field, which was derived from the location of the peaks in  $\chi''(T)$  or  $\chi''(f)$ . The squares come from  $\chi''(T)$  curves such as those of Fig. 2(a) [ $\tau(T_{\max})=1/2\pi f$ ]; the circles come from  $\chi''(f)$  curves such as those of Fig. 2(b) [ $\tau(T)=1/2\pi f_{\max}$ ]; and the diamonds from  $\chi''(f)$  curves recorded after either 0, 2, or 4 h, such as in Fig. 3. The solid line shows the Arrhenius regime, while the dashed line corresponds to the quantum regime associated with a constant relaxation time  $\tau_S \sim 0.4$  s.

are also observed at lower temperatures (i.e., in the range 2–6 K), in a regime where no sizable relaxation effect was detected. Experimental results indicate that this behavior are not associated with the fact that the data are collected versus  $T$  or  $f$ , but is instead an effect that is related to the cooling rate value. We have checked that the cooling rates used to record the  $\chi''(T)$  curves do indeed influence the  $\chi''$  values at low  $T$ . At 1 Hz, for instance, a  $\chi''(T)$  curve recorded with a fast cooling leads to values at low  $T$  (i.e., in the 2–6 K range) that are as large as those found in Fig. 2(b). For this low- $T$  range, it thus appears that the cooling rate should be regarded as a parameter affecting the preparation of the magnetic system. For any disordered (or partially disordered) ground state, it is known that the rate at which the system crosses the freezing temperature is an important parameter. In our case, the cooling rate can thus be expected to affect the frozen-spin state ( $T < T_{\text{SF}} \sim 7\text{--}8$  K) and thereby its magnetic response (in particular  $\chi''$ ). In the next section, we will come back to these effects of the cooling rate.

From the location of the peaks in the  $\chi''(T)$  or  $\chi''(f)$  curves, we extracted the temperature dependence of the spin-relaxation time,  $\tau(T)=1/2\pi f$ . The results are shown in a  $\tau$  vs  $1/T$  plot in Fig. 4. At the highest temperatures, there is an Arrhenius regime of the form  $\tau=\tau_0 \exp(\Delta/T)$ , where the best fit gives  $\tau_0 \sim 2 \times 10^{-8}$  s and  $\Delta \sim 135$  K. As  $T$  is decreased, the data exhibit a splitting into two branches: one branch appears as an extrapolation of the Arrhenius regime found at higher  $T$ , while the second corresponds to the emergence of a temperature-independent spin-relaxation time  $\tau_S \sim 0.4$  s.

The shape of  $\chi''(f)$  at the lowest  $T$ , however, shows that we are not simply dealing with one characteristic time. For instance, the peak in  $\chi''(f)$  at 2.25 K displayed in Fig. 5 is broader than the expectation for a single relaxation time (i.e., a half width at half maximum close to 0.57 decades in

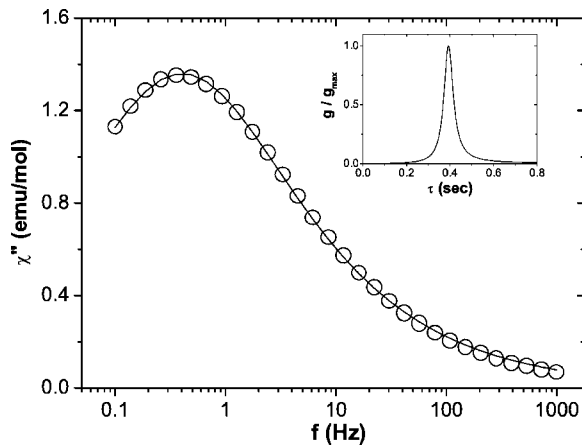


FIG. 5.  $\chi''(f)$  in zero field at 2.25 K. The solid line is a fit to the data assuming the existence of a distribution function  $g(\tau)$  in the  $\tau$  values (see text). A normalized plot of this function is shown in the inset.

frequency).<sup>29</sup> We also checked that the Argand plot ( $\chi''$  vs  $\chi'$ ) displays a flattened portion instead of the perfect semi-circle expected for a single characteristic time.<sup>28</sup> Whatever the nature of the dissipation mechanism, such features can be ascribed to the existence of a distribution  $g(\tau)$  in the values of the characteristic time. Using the analysis proposed by Hüser *et al.* for spin glasses,<sup>30</sup> the width of the distribution around  $\tau_S$  is characterized by a parameter  $\alpha$  (whose value increases from 0 to 1 as the width varies from zero to infinity) leading to

$$\chi''(f) \propto \frac{\cos(\alpha\pi/2)}{\cosh[(1-\alpha)\ln(2\pi f\tau_S)] + \sin(\alpha\pi/2)}.$$

The best fit to the data at  $T=2.25$  K (see Fig. 5) gives  $\alpha \sim 0.55$ . This value corresponds to the distribution function  $g(\tau)$  shown in the inset of Fig. 5.

We have also noted an anomaly in the evolution of the shape of  $\chi''(f)$  as a function of  $T$ : Fig. 6 shows normalized curves of  $\chi''/\chi''_{\max}$  vs  $f/f_{\max}$  at three temperatures around the splitting point in Fig. 4. One observes that the curve at 10 K is very symmetrical whereas a distortion takes place between the  $f > f_{\max}$  and  $f < f_{\max}$  portions of the curves as  $T$  is reduced. This asymmetry is found to be maximal at  $T \sim 7$  K. The lower panel of Fig. 6 shows the  $\chi''(f)$  data at 7 K along with the theoretical  $\chi''(f)$  curve ( $\alpha=0.53$ ) obtained when fitting the data for  $f > f_{\max}$ . The shift appearing for  $f < f_{\max}$  between the experimental and calculated curves can be accounted for by considering that a smooth peak centered around 0.03 Hz is superimposed onto a symmetrical bell-like curve. Such a behavior suggests the presence of two maxima in  $\chi''(f)$ , i.e., the existence of a competition between two dissipation mechanisms in a certain temperature range. It should be emphasized that such a feature is in agreement with the coexistence of two branches in Fig. 4. From a quantitative point of view, it must also be noted that the location of the broad maximum at  $f \sim 0.03$  Hz leads to  $\tau \sim 5$  s at  $T = 7$  K, which gives a point lying on the “Arrhenius-like branch” at  $T < T_{\text{cross}}$  (see Fig. 4).

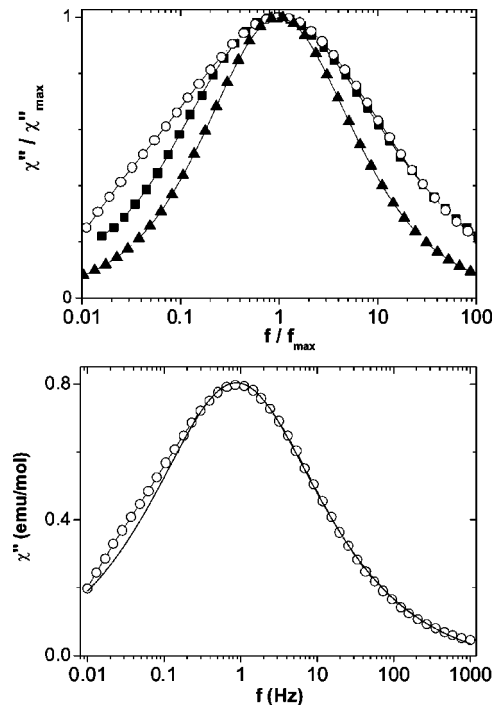


FIG. 6. Top panel: Normalized frequency dependence of  $\chi''$  in zero field at 10 K (solid triangles), 7 K (open circles), and 5 K (solid squares). Bottom panel:  $\chi''(f)$  curve in zero field at  $T=7$  K. The solid line is the theoretical curve derived from a fit to the data for  $f > f_{\max}$ .

The second part of our work was devoted to a study of the influence of dc magnetic fields on the dissipative behavior at low temperatures. We performed this study at  $T=2$  K, a temperature at which the  $M(H)$  curve exhibits steps for regularly spaced values of  $H$ , in particular for 0, 1.2, and 2.4 T.<sup>21</sup> The dynamical character of these magnetization steps is supported by the fact that they cannot be clearly detected when using magnetic-field sweep rates that are too large.<sup>10</sup> Figure 7 shows  $\chi''(f)$  curves that were recorded at 2 K in several dc magnetic fields ranging from 0 to 2.6 T. This series of

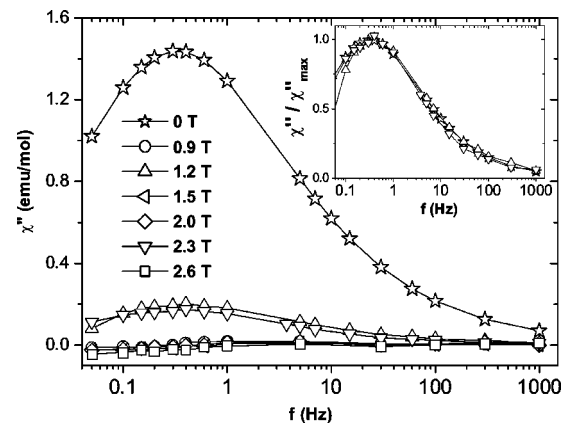


FIG. 7.  $\chi''(f)$  curves at 2 K in a series of magnetic fields applied along the  $c$  axis. The inset shows rescaled curves for 0 T (stars), 1.2 T (triangles up), and 2.3 T (triangles down).

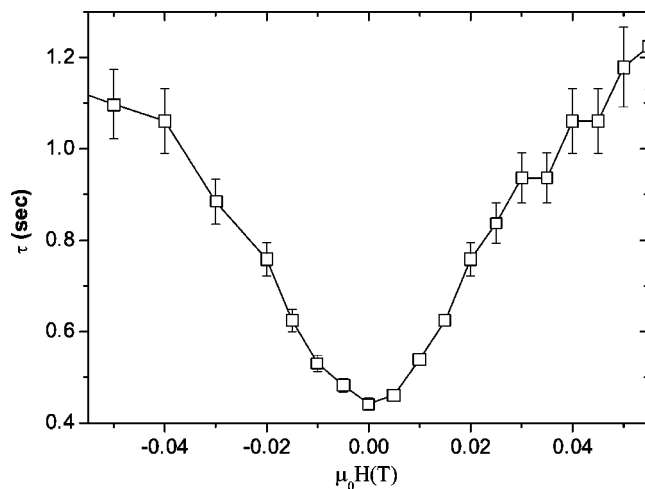


FIG. 8. Field dependence of  $\tau$  at  $T=2$  K. The data were derived from the location of the maximum in  $\chi''(f)$  curves [ $\tau(H) = 1/2\pi f_{\max}(H)$ ].

curves reveals a strongly nonmonotonic evolution of the shape of  $\chi''(f)$  as  $H$  is increased. The most salient feature is that the curves recorded in 1.2 and 2.3 T (i.e., close to step fields) clearly differ from those obtained in the other fields. The inset displays the  $\chi''/\chi''_{\max}$  vs  $f$  curves for  $\mu_0 H=0, 1.2$ , and 2.3 T. This scaling shows that the characteristic spin-relaxation time as well as the global shape of  $\chi''(f)$  are almost the same for these three fields. In the other magnetic fields, the  $\chi''$  values are very small. With a SQUID-based ac susceptometer as presently used, we note that the combination of large dc field, low temperature, and low frequency favors the appearance of significant phase shifts which cannot be easily corrected when the amplitude of the signal is too small.<sup>31</sup> This feature hindered a precise analysis of the  $\chi''(f)$  curves (and in particular an estimate of the characteristic spin-relaxation time) recorded in large magnetic fields well away from the resonances.

Fortunately,  $\mu_0 H=0$  T is expected to be a resonant field within the framework of QTM theory.<sup>22</sup> In this case, one can use values of  $H$  that remain small enough to allow a quantitative analysis of  $\chi''(f)$  and the derivation of  $\tau(H)$ . At  $T=2$  K,  $\chi''(f)$  curves were recorded in a series of magnetic fields around  $\mu_0 H=0$  T (for these measurements, we used a linear frequency increment of  $\sim 0.017$  Hz). Figure 8 shows the  $\tau$  values derived from the location of the maximum in  $\chi''(f)$ , i.e.,  $\tau(H)=1/2\pi f_{\max}(H)$ . The key point is that  $\tau(H)$  exhibits a clear dip at  $\mu_0 H=0$  T, as is expected for a QTM process around a resonant field.<sup>22-24</sup>

#### IV. DISCUSSION

Previous studies have reported ac susceptibility measurements in  $\text{Ca}_3\text{Co}_2\text{O}_6$  (Refs. 8, 13, and 21) and related compounds, such as  $\text{Ca}_3\text{CoRhO}_6$  (Ref. 32) and  $\text{Ca}_3\text{CoIrO}_6$ .<sup>33</sup> They demonstrated the existence of a slow spin relaxation at low temperatures, with a large frequency dependence of the maximum ( $T_{\max}$ ) of  $\chi''(T)$ . In  $\text{Ca}_3\text{Co}_2\text{O}_6$ , the parameter

$(\Delta T_{\max}/T_{\max})/\Delta \log_{10} f$  was found to be  $\sim 0.17$ ,<sup>8</sup> which is much larger than the expectation for a standard spin glass.<sup>28</sup> Such a value points to a superparamagnetic behavior, as suggested earlier by Maignan *et al.* in their single-crystal study.<sup>8</sup> In  $\text{Ca}_3\text{CoRhO}_6$ , Sampathkumaran *et al.* also reported results typical of the dynamics of superparamagnetic clusters for  $T < T_N$ , as well as the existence of a spin-freezing phenomenon at a lower temperature ( $T_{\text{SF}}$ ).<sup>32</sup> Other experimental results, however, were found to remain consistent with a spin-glass-like behavior, suggesting the existence of an “exotic” spin-glass state, including in the case of  $\text{Ca}_3\text{Co}_2\text{O}_6$ .<sup>13</sup>

More recently, an investigation of the spin dynamics in  $\text{Ca}_3\text{Co}_2\text{O}_6$  crystals (down to temperatures lower than those of the previous studies) has revealed a saturation of the spin-relaxation time.<sup>21</sup> This feature, however, emerged from the combination of two types of measurements: ac susceptibility [ $\chi''(T)$ ] and dc relaxation of the magnetization [ $M(t)$ ]. In the present work, the temperature dependence of the spin-relaxation time is derived only from the analysis of  $\chi''$  data, over the whole  $T$  range down to 2 K. These results clearly confirm that, as  $T$  decreases,  $\tau(T)$  shows an Arrhenius regime followed by a saturation to a constant value  $\tau_S$ . The crossover between these activated and quantumlike regimes takes place at  $T_{\text{cross}} \sim 8$  K, i.e., close to the spin-freezing temperature  $T_{\text{SF}}$  found in magnetization and specific heat studies.<sup>6,11,12</sup> The data of Fig. 4 are in good agreement with our previous study except about the value of  $\tau_S$ : it is  $\sim 0.4$  s in the present study, while it was reported to be  $\sim 1000$  s in the previous one.<sup>21</sup> We emphasize, however, that this previous value was derived from the analysis of dc relaxation curves, using a model-dependent expression for  $M(t/\tau)$ . In contrast, the  $\tau(T)$  values of the present work were derived from a direct analysis of  $\chi''$  over the whole  $T$  range, which makes the value  $\tau_S \sim 0.4$  s more reliable.

Another finding of the present study is the overlap between the Arrhenius regime and the emergence of a  $T$ -independent spin-relaxation time. We stress that the coexistence of activated and quantum regimes of relaxation is not unexpected from a theoretical point of view.<sup>22</sup> To date, however, such a behavior has not been reported in the widely investigated SMM's. In  $\text{Ca}_3\text{Co}_2\text{O}_6$ , this coexistence of both over- and underbarrier mechanisms ( $T$  dependent and  $T$  independent, respectively) generates two diverging branches below  $T_{\text{cross}} \sim 8$  K on the  $\tau$  vs  $1/T$  plot. It is worth noticing that Snyder *et al.*<sup>26</sup> have recently emphasized a related feature in their study of the geometrically frustrated pyrochlore  $\text{Dy}_2\text{Ti}_2\text{O}_7$ . These authors did note the existence of a broad bump coexisting with a sharper peak on the  $\chi''(f)$  curve at  $T=12$  K  $\leq T_{\text{cross}}=13$  K. This behavior clearly bears a close similarity with the results found at  $T=7$  K  $\leq T_{\text{cross}}=8$  K in  $\text{Ca}_3\text{Co}_2\text{O}_6$ .

Within the Arrhenius regime [ $\tau=\tau_0 \exp(\Delta/T)$ ], the values of  $\tau_0$  ( $2 \times 10^{-8}$  s) and  $\Delta$  (135 K) in  $\text{Ca}_3\text{Co}_2\text{O}_6$  are not very different from those reported in SMM's. For instance,  $\tau_0 \sim 2 \times 10^{-7}$  s and  $\Delta \sim 60$  K in  $\text{Mn}_{12}$ . However, this may be coincidental since  $\text{Ca}_3\text{Co}_2\text{O}_6$  corresponds to a very different magnetic situation. In  $\text{Ca}_3\text{Co}_2\text{O}_6$ , the superparamagnetic regime involves Ising-like spin chains with a ferromagnetic intrachain coupling, in addition to the single-ion anisotropy.

In a recent paper addressing this particular situation,<sup>34</sup> it was found that  $\Delta$  depends on both  $J$  and  $D$ . In the case of  $\text{Ca}_3\text{Co}_2\text{O}_6$ , a direct determination of  $D$  by independent measurements (e.g., electronic paramagnetic resonance or inelastic neutron scattering) is not yet available, which prevents us from making a reliable quantitative analysis of the  $\Delta$  value. Coulon *et al.* have also shown that finite-size effects related to the presence of defects can induce a crossover within the activated regime of single-chain magnets combining single-ion anisotropy and ferromagnetic coupling.<sup>34</sup> In our case (see Fig. 4), we have no indication of such a crossover within the purely activated regime ( $T > T_{\text{cross}}$ ), while the apparent change in slope of  $\ln \tau$  vs  $1/T$  below  $T_{\text{cross}}$  (down to  $\sim 4$  K) is too large to be consistent with the expectations of Ref. 34 (i.e., much larger than a factor of 2). To investigate the possible occurrence of a crossover related to defects in  $\text{Ca}_3\text{Co}_2\text{O}_6$ , measurements should be carried out at larger frequencies in order to access the activated regime over a wider range of temperatures ( $T > 13$  K).

In other respects, the value of  $\tau_S$  found in  $\text{Ca}_3\text{Co}_2\text{O}_6$  is much smaller than all the results reported for SMM's. In  $\text{Mn}_{12}$ , for instance,  $\tau_S$  is estimated to be about  $10^9$  s, while it is of the order of  $10^5$  s in  $\text{Fe}_8$ .<sup>24</sup> On the other hand,  $\tau_S \sim 0.4$  s is larger than the value  $\sim 0.005$  s reported for  $\text{Dy}_2\text{Ti}_2\text{O}_7$ .<sup>26</sup> It is difficult to account for these huge differences between materials, since the expected values for  $\tau_S$  are strongly dependent on the perturbative terms of the Hamiltonian, which determine the tunneling process (higher-order spin term, transverse field, spin-phonon interactions, etc.).<sup>22,24</sup> It turns out that the nature of the additional interaction which governs  $\tau_S$  cannot be easily identified (even in the widely investigated SMM's this issue is still intensively debated). Furthermore, we cannot expect *a priori* that this mechanism will be the same for SMM's and for one- or three-dimensional geometrically frustrated oxides.

Another striking result displayed by the ac susceptibility data of  $\text{Ca}_3\text{Co}_2\text{O}_6$  is the pronounced time dependence of  $\chi''(f)$  in a particular  $T$  range ( $\sim 10 \pm 2$  K). It should be emphasized that a drastic influence of the waiting time in magnetization measurements has been observed within the same  $T$  range.<sup>11</sup> With the crystals of the present study, we confirmed that the dc relaxation in low fields (5 Oe) is particularly pronounced around 10 K (variation of  $M$  by  $\sim 50\%$  over 4 h). The location of this  $T$  range near  $T_{\text{cross}} \sim 8$  K suggests that this time effect may be related to the competition between the activated and quantum regimes. However, the way these mechanisms interact together to give rise to such an unusual relaxation effect remains unclear at the present time. The influence of the cooling rate on the  $\chi''$  values in the low- $T$  range ( $T \leq 6$  K) is another phenomenon which needs to be clarified. We suggest that it may be related to the fact that the cooling rate throughout the spin-freezing process (i.e., around  $T_{\text{SF}} \sim 7-8$  K) is able to modify the degree of disorder in the magnetic state at low  $T$ . We note that the impact on  $\chi''$  is quite complex since it is found to depend on the characteristic time of the measurement ( $\tau_m = 1/2\pi f$ ) with respect to the characteristic spin-relaxation time associated with QTM ( $\tau_S \sim 0.4$  s). The  $\chi''$  values observed at low  $T$  are largest for the “fast cooling” preparation [ $\chi''(f)$  curves]

at 10 and 1 Hz (i.e.,  $\tau_m < \tau_S$ ), whereas they are largest for the “slow cooling” preparation [ $\chi''(T)$  curves] at 0.1 and 0.01 Hz (i.e.,  $\tau_m > \tau_S$ ). This apparent interplay between the cooling rate,  $\tau_m$ , and  $\tau_S$  will have to be investigated in more detail.

The similarity between the  $\chi''(f)$  curves recorded at 2 K in 0, 1.2, and 2.3 T points to the same dissipative mechanism for the fields corresponding to the steps in the  $M(H)$  data, whereas the curves in intermediate fields are very different. Such behavior adds further strong support to the existence of QTM in  $\text{Ca}_3\text{Co}_2\text{O}_6$ . Within the framework of QTM theory, the magnetization steps originate from a decrease in  $\tau$  when the field is equal to a resonant value [ $\mu_0 H = n(D/g\mu_B)$ ].<sup>22</sup> Our investigation of the field dependence of  $\tau$  showed a clear dip at  $\mu_0 H = 0$  T, exactly as expected for a QTM process since zero field is a resonant field ( $n=0$ ). We note that the analysis of ac susceptibility data in  $\text{Mn}_{12}$  led to the same behavior.<sup>35</sup> In  $\text{Mn}_{12}$ , the dip in zero field yields a variation in  $\tau$  by about a factor of 5 over a width of  $\sim 0.2$  T. Even quantitatively, the results in  $\text{Ca}_3\text{Co}_2\text{O}_6$  are comparable since  $\tau$  varies by about a factor of 3 over a width of  $\sim 0.1$  T. With such a typical width for the QTM process around each step field, one can estimate that the magnetization steps in  $M(H)$  should hardly develop for sweep rates much larger than  $\sim 0.1$  T/ $\tau_S = 0.25$  T/s. This rough estimate turns out to be compatible with the fact that the characteristic steps close to 1.2 and 2.4 T at  $T=2$  K were clearly visible in our measurements by means of a vibrating sample magnetometer (including for the largest sweep rate equal to 0.017 T/s),<sup>21</sup> while they were difficult to detect in pulsed-field experiments (the lowest sweep rate being 5 T/s).<sup>10</sup>

## V. CONCLUSION

The spin dynamics of  $\text{Ca}_3\text{Co}_2\text{O}_6$  have been investigated by analyzing the dissipative component of the ac magnetic susceptibility. In zero field, the temperature dependence of the spin-relaxation time ( $\tau$ ) shows a crossover between an activated (Arrhenius-like) regime and a quantum ( $T$ -independent) regime, around  $T_{\text{cross}} \sim 8$  K. This behavior is consistent with a QTM process. Moreover, the influence of the magnetic field on the spin dynamics at low  $T$  is also found to be consistent with the expectations for a QTM process: (i) the dissipation mechanism is the same in magnetic fields corresponding to magnetization steps on  $M(H)$ ; (ii)  $\tau(H)$  exhibits a dip at  $\mu_0 H = 0$  T.

Therefore, the present study adds further support to the view that QTM occurs in  $\text{Ca}_3\text{Co}_2\text{O}_6$ . This spin-chain compound can thus be regarded as an example of a geometrically frustrated material exhibiting a QTM-like process.<sup>25,26</sup> In  $\text{Ca}_3\text{Co}_2\text{O}_6$ , the magnetic centers undergoing QTM should reside within the incoherent chains of the PDA state. The basic units are the high-spin  $\text{Co}^{3+}$  ( $S=2$ ) but macrospins made up of  $n$  ferromagnetically coupled neighbors ( $S=2n$ ) may also play a role.<sup>21</sup> This issue remains to be clarified.

In  $\text{Ca}_3\text{Co}_2\text{O}_6$ , the spin-relaxation time of the quantum regime ( $\tau_S \sim 0.4$  s) is found to be much smaller than in single-molecular magnets;  $\tau_S$  lies within a time window that is well

suiting to experiments. This small value of  $\tau_S$  also contributes to the fact that the quantum regime extends up to rather high temperatures in  $\text{Ca}_3\text{Co}_2\text{O}_6$  ( $T_{\text{cross}} \sim 8$  K), which is another advantage from an experimental viewpoint. In conclusion,

we emphasize that the recent results found in  $\text{Ca}_3\text{Co}_2\text{O}_6$  and  $\text{Dy}_2\text{Ti}_2\text{O}_7$  (Ref. 26) encourage a wider investigation of the occurrence of QTM in other geometrically frustrated magnetic oxides.

- <sup>1</sup>*Magnetic Systems with Competing Interactions*, edited by H. T. Diep (World Scientific, Singapore, 1994); P. Schiffer and A. P. Ramirez, *Comments Condens. Matter Phys.* **18**, 21 (1996); A. P. Ramirez, in *Handbook of Magnetic Materials*, edited by K. J. H. Buschow (Elsevier, Amsterdam, 2001); S. T. Bramwell and M. P. Gingras, *Science* **294**, 1495 (2001).
- <sup>2</sup>M. F. Collins and O. A. Petrenko, *Can. J. Phys.* **75**, 605 (1997).
- <sup>3</sup>K. E. Stitzer, J. Darriet, and H.-C. zur Loye, *Curr. Opin. Solid State Mater. Sci.* **5**, 535 (2001).
- <sup>4</sup>H. Fjellvag, E. Gulbrandsen, S. Aasland, A. Olsen, and B. Hauback, *J. Solid State Chem.* **124**, 190 (1996).
- <sup>5</sup>S. Aasland, H. Fjellvag, and B. Hauback, *Solid State Commun.* **101**, 187 (1997).
- <sup>6</sup>H. Kageyama, K. Yoshimura, K. Kosuge, H. Mitamura, and T. Goto, *J. Phys. Soc. Jpn.* **66**, 1607 (1997).
- <sup>7</sup>H. Kageyama, K. Yoshimura, K. Kosuge, M. Azuma, M. Takano, H. Mitamura, and T. Goto, *J. Phys. Soc. Jpn.* **66**, 3996 (1997).
- <sup>8</sup>A. Maignan, C. Michel, A. C. Masset, C. Martin, and B. Raveau, *Eur. Phys. J. B* **15**, 657 (2000).
- <sup>9</sup>B. Martínez, V. Laukhin, M. Hernando, J. Fontcuberta, M. Parras, and J. M. González-Calbet, *Phys. Rev. B* **64**, 012417 (2001).
- <sup>10</sup>B. Raquet, M. N. Baibich, J. M. Broto, H. Rakoto, S. Lambert, and A. Maignan, *Phys. Rev. B* **65**, 104442 (2002).
- <sup>11</sup>V. Hardy, S. Lambert, M. R. Lees, and D. McK. Paul, *Phys. Rev. B* **68**, 014424 (2003).
- <sup>12</sup>V. Hardy, M. R. Lees, A. Maignan, S. Hébert, D. Flahaut, C. Martin, and D. McK. Paul, *J. Phys.: Condens. Matter* **15**, 5737 (2003).
- <sup>13</sup>S. Rayaprol, K. Sengupta, and E. V. Sampathkumaran, *Solid State Commun.* **128**, 79 (2003).
- <sup>14</sup>R. Frésard, C. Laschinger, T. Kopp, and V. Eyert, *Phys. Rev. B* **69**, 140405(R) (2004).
- <sup>15</sup>E. V. Sampathkumaran, N. Fujiwara, S. Rayaprol, P. K. Madhu, and Y. Uwatoko, *Phys. Rev. B* **70**, 014437 (2004).
- <sup>16</sup>V. Hardy, M. R. Lees, O. A. Petrenko, D. McK. Paul, D. Flahaut, S. Hébert, and A. Maignan, *Phys. Rev. B* **70**, 064424 (2004).
- <sup>17</sup>D. Flahaut, A. Maignan, S. Hébert, C. Martin, R. Retoux, and V. Hardy, *Phys. Rev. B* **70**, 094418 (2004).
- <sup>18</sup>M. H. Whangbo, D. Dai, H. J. Koo, and S. Jovic, *Solid State Commun.* **125**, 413 (2003).
- <sup>19</sup>S. Niitaka, K. Yoshimura, K. Kosuge, M. Nishi, and K. Kakurai, *Phys. Rev. Lett.* **87**, 177202 (2001).
- <sup>20</sup>M. Mekata, *J. Phys. Soc. Jpn.* **42**, 76 (1977); M. Mekata and K. Adachi, *ibid.* **44**, 806 (1978).
- <sup>21</sup>A. Maignan, V. Hardy, S. Hébert, M. Drillon, M. R. Lees, O. Petrenko, D. McK. Paul, and D. Khomskii, *J. Mater. Chem.* **14**, 1231 (2004).
- <sup>22</sup>For a review, see *Quantum Tunneling of Magnetization*, edited by L. Gunther and B. Barbara (Kluwer, Dordrecht, 1995).
- <sup>23</sup>R. Sessoli, D. Gatteschi, A. Caneschi, and M. A. Novak, *Nature (London)* **365**, 141 (1993); B. Barbara, W. Wernsdorfer, L. C. Sampaio, J. G. Park, C. Paulsen, M. A. Novak, R. Ferré, D. Maily, R. Sessoli, A. Caneschi, K. Hasselbach, A. Benoit, and L. Thomas, *J. Magn. Magn. Mater.* **140–144**, 1825 (1995); J. R. Friedman, M. P. Sarachik, J. Tejada, and R. Ziolo, *Phys. Rev. Lett.* **76**, 3830 (1996); L. Thomas, F. Lioni, R. Ballou, D. Gatteschi, R. Sessoli, and B. Barbara, *Nature (London)* **383**, 145 (1996); E. M. Chudnovsky, *Science* **274**, 938 (1996); J. M. Hernandez, X. X. Zhang, F. Luis, J. Tejada, J. R. Friedman, M. P. Sarachik, and R. Ziolo, *Phys. Rev. B* **55**, 5858 (1997).
- <sup>24</sup>D. Gatteschi and R. Sessoli, *Angew. Chem., Int. Ed.* **42**, 268 (2003).
- <sup>25</sup>G. Ehlers, A. L. Cornelius, M. Orendac, M. Kajnakova, T. Fennell, S. T. Bramwell, and J. S. Gardner, *J. Phys.: Condens. Matter* **15**, L9 (2003).
- <sup>26</sup>J. Snyder, B. G. Ueland, J. S. Slusky, H. Karunadasa, R. J. Cava, A. Mizel, and P. Schiffer, *Phys. Rev. Lett.* **91**, 107201 (2003).
- <sup>27</sup>M. Loewenhaupt, W. Schäfer, A. Niazi, and E. V. Sampathkumaran, *Europhys. Lett.* **63**, 374 (2003).
- <sup>28</sup>J. A. Mydosh, *Spin Glasses: An Experimental Introduction* (Taylor and Francis, London, 1993).
- <sup>29</sup>J. Snyder, J. S. Slusky, R. J. Cava, and P. Schiffer, *Phys. Rev. B* **66**, 064432 (2002).
- <sup>30</sup>D. Hüser, A. J. van Duynveldt, G. J. Nieuwenhuys, and J. A. Mydosh, *J. Phys. C* **19**, 3697 (1986).
- <sup>31</sup>A. D. Hibbs, R. E. Sager, S. Kumar, J. E. McArthur, A. L. Singaas, K. G. Jensen, M. A. Steindorf, T. A. Aukerman, and H. M. Schneider, *Rev. Sci. Instrum.* **65**, 2644 (1994).
- <sup>32</sup>E. V. Sampathkumaran and A. Niazi, *Phys. Rev. B* **65**, 180401(R) (2002).
- <sup>33</sup>S. Rayaprol, K. Sengupta, and E. V. Sampathkumaran, *Phys. Rev. B* **67**, 180404(R) (2003).
- <sup>34</sup>C. Coulon, R. Clérac, L. Lecren, W. Wernsdorfer, and H. Miyasaka, *Phys. Rev. B* **69**, 132408 (2004).
- <sup>35</sup>F. Luis, J. Bartolomé, J. F. Fernandez, J. Tejada, J. M. Hernandez, X. X. Zhang, and R. Ziolo, *Phys. Rev. B* **55**, 11 448 (1997).